Antiviral Research 97 (2013) 334–346

Contents lists available at SciVerse ScienceDirect

Antiviral Research

journal homepage: www.elsevier.com/locate/antiviral

Spray drying tenofovir loaded mucoadhesive and pH-sensitive microspheres intended for HIV prevention

Tao Zhang [a], Chi Zhang [b], Vivek Agrahari [a], James B. Murowchick [c], Nathan A. Oyler [b], Bi-Botti C. Youan [a,*]

[a] Laboratory of Future Nanomedicines and Theoretical Chronopharmaceutics, Division of Pharmaceutical Science, University of Missouri-Kansas City, Kansas City, MO 64108, United States
[b] Department of Chemistry, University of Missouri-Kansas City, Kansas City, MO 64110, United States
[c] Department of Geosciences, University of Missouri-Kansas City, Kansas City, MO 64110, United States

ARTICLE INFO

Article history:
Received 22 May 2012
Revised 13 December 2012
Accepted 18 December 2012
Available online 26 December 2012

Keywords:
pH-sensitive
Mucoadhesive
Tenofovir
Spray drying
HIV/AIDS microbicide

ABSTRACT

Purpose: To develop spray dried mucoadhesive and pH-sensitive microspheres (MS) based on polymethacrylate salt intended for vaginal delivery of tenofovir (a model HIV microbicide) and assess their critical biological responses.
Methods: The formulation variables and process parameters are screened and optimized using a 2^{4-1} fractional factorial design. The MS are characterized for size, zeta potential, yield, encapsulation efficiency, Carr's index, drug loading, *in vitro* release, cytotoxicity, inflammatory responses and mucoadhesion.
Results: The optimal MS formulation has an average size of 4.73 μm, zeta potential of −26.3 mV, 68.9% yield, encapsulation efficiency of 88.7%, Carr's index of 28.3 and drug loading of 2% (w/w). The MS formulation release 91.7% of its payload in the presence of simulated human semen. At a concentration of 1 mg/ml, the MS are noncytotoxic to vaginal endocervical/epithelial cells and *Lactobacillus crispatus* when compared to control media. There is also no statistically significant level of inflammatory cytokine (IL1-α, IL-1β, IL-6, IL-8, and IP-10) release triggered by these MS. Their percent mucoadhesion is 2-fold higher than that of 1% HEC gel formulation.
Conclusion: These data suggest the promise of using such MS as an alternative controlled microbicide delivery template by intravaginal route for HIV prevention.

1. Introduction

HIV/AIDS remains the deadliest epidemic of our time. In the 2011 UNAIDS global report, WHO estimated there were 2.7 million new infections and 1.8 million AIDS related deaths in 2010 (UNAIDS/WHO, 2011). Unprotected, heterosexual, vaginal intercourse is still one of the major routes of infection. In sub-Saharan Africa, which is identified as the region where most new infections occur, women constitute about 60% of the total population that is living with HIV (2010). To this date alternative pre-exposure prophylaxis (PrEP) methods are urgently needed, given that antiretroviral therapy is still far from curing the disease and a successful HIV vaccine is yet to be developed. The idea of PrEP methods started with the oral application of antiretroviral drugs, and later focused on the vaginal/rectal application of anti-HIV substances, known as microbicides. A great variety of HIV microbicides candidates have been studied and tested (das Neves et al., 2011; Mbopi-Keou et al., 2010; McCormack et al., 2010; Wan et al., 2007). In terms of formulation, a lot of the emphasis has been put on the first generation gel formulation, and some positive results have been shown (Garg et al., 2010). In the CAPRISA004 trial, in which a 1% tenofovir gel was tested, HIV incidence was reduced by 54% in the high gel adherence (>80%) group (Karim et al., 2010). This promising result shed light on the prospect of a possible total protection against HIV, if a sustainable concentration of the active drug can be maintained. Meanwhile the TFV gel arm was terminated for futility in VOICE HIV prevention trials indicating that the differences in dosing strategies is important in the outcomes of the prevention (FHI, 2011). However, such an aqueous gel system suffers from several disadvantages, the most significant one being its low retention time within the vaginal cavity, which requires a high dosing frequency (Karim et al., 2010). Such "before and after sex" dosing strategy (otherwise regarded as "coital dependence" (Morrow and Ruiz, 2008) sometimes leads to poor acceptability and adherence. An ideal prevention strategy for women at high-risk of sexually-acquired HIV could be the use of

* Corresponding author. Address: Laboratory of Future Nanomedicine and Theoretical Chronopharmaceutics, Division of Pharmaceutical Science, University of Missouri-Kansas City, 2464 Charlotte, Kansas City, MO 64108, United States. Tel.: +1 816 235 2410; fax: +1 816 235 5779.
E-mail addresses: youanb@mail.umkc.edu, youanbi@yahoo.com (Bi-B.C. Youan).

0166-3542/$ - see front matter © 2013 Elsevier B.V. All rights reserved.
http://dx.doi.org/10.1016/j.antiviral.2012.12.019

a microbicide formulation that could be administered in a coital-independent fashion (e.g. once a day). To achieve this goal, the ideal formulation should (a) have high vaginal retention time, and (b) be able to release a high dose of microbicide when sexual intercourse occurs.

So far, there isn't much literature on the development of a second generation topical microbicide formulation incorporating a triggering-release mechanism, although many concerns have been given to safe delivery of microbicides using nanotechnology (Whaley et al., 2010). In a pilot study, Gupta et al., 2007 demonstrated a temperature and pH-sensitive hydrogel taking advantage of the drastic pH change in the presence of human semen as a triggering factor for the burst release of the microbicide (Gupta et al., 2007). Most recently, Mahalingam et al., 2011 developed a pH-sensitive mucin like polymer that could significantly impede HIV migration at pH $\geqslant$ 4.8 (Mahalingam et al., 2011 and Clark et al., 2011) reported an enzymatic triggered release of HIV-entry inhibitors (Clark et al., 2011). It has recently been shown that PLGA/Eudragit S-100 blend nanoparticle loaded with tenofovir can have a 4-fold increase in the release rate in the presence of semen and is noncytotoxic to vagina epithelium and vaginal flora (Zhang et al., 2011).

This study reports for the first time the development of a spray dried mucoadhesive and pH-sensitive microspheres (MS) formulation, based on polymethacrylate salt intended for vaginal delivery of HIV microbicides. It has been shown that the sodium or potassium salts of the methacrylic copolymers Eudragit L-100 and S-100 have the potential as a novel low-swellable mucoadhesive material (Cilurzo et al., 2003, 2005). We postulate that a topical formulation prepared from sodium salt of Eudragit S-100 (EuSNa) may provide site-retentive characteristics as well as pH-sensitive release, which could be a potential alternative solution to current gel formulation. In this study, tenofovir was formulated into a spray dried EuSNa microparticle (EuSNa-MS) formulation. This study encompasses the formulation optimization, characterization, *in vitro* safety, *in vitro* mucoadhesion, and immunogenicity testing.

2. Materials and methods

2.1. Materials

The Tenofovir (TFV) was purchased from Zhongshuo Pharmaceutical Co. Ltd. (Beijing, China). The Eudragit® S-100 (Methacrylic acid-methyl methacrylate copolymer 1:2) was purchased from Evonik Industries (Darmstadt, Germany). The sodium hydroxide was purchased from Sigma–Aldrich (St. Louis, MO, USA). The Oregon green® 488 cadaverin *5-isomer* was purchased from Invitrogen Corp. (Carlsbad, CA, USA). The CytoTox-ONE™ and CellTiter 96™ Aqueous kits were purchased from Promega (Madison, WI, USA). The Milliplex MAP multiplex assay kits were purchased from Millipore (Billerica, MA, USA). All other chemicals used in this study were of analytical grade and used without further purification.

2.2. Experimental design

In this study, a 2^{4-1} fractional factorial experimental design was used to study the effect of four formulation variables, namely, polymer concentration, polymer to drug ratio, inlet temperature, feed flow rate on drug encapsulation efficiency, yield, and Carr's index. These independent and dependent variables, and their coded factors, are listed in Table 1. All independent variables in this study were chosen based on preliminary experiments (data not shown).

Table 1
Variables and their levels in 2^{4-1} design.

	Levels		
	Low	High	Centerpoints
Independent variables			
X_1 = Polymer concentration (%)	2	5	3.5
X_2 = Polymer: drug	10	40	25
X_3 = Inlet temperature (°C)	100	140	120
X_4 = Feed flow rate (ml/min)	1.6	6.4	4.0
Coded values (X_1, X_2, X_3, X_4)	−	+	0
Dependent variables			
Y_1 = Drug encapsulation efficiency (%)			
Y_2 = Yield (%)			
Y_3 = Carr's index (%)			

2.3. Microspheres preparation

Eudragit S-100 sodium salt (EuSNa) was prepared according to the method adopted from Cilurzo et al., 2003. Briefly, Eudragit S-100 (S-100) was dissolved in water containing sodium hydroxide (NaOH) pellets to assure complete salification. The ratio of S-100 to NaOH was calculated based on the acid value of the S-100 (Degussa, 2011). The solution was spray dried as described below.

To prepare tenofovir-loaded EuSNa microspheres (EuSNa-TFV MS), different amounts of S-100 and TFV were added in 20 ml of deionized water with an appropriate amount of NaOH to achieve complete salification. The solution was then spray dried using a Buchi Mini Spray Dryer, Model 290 (Buchi Laboratoriums - Technik AG, Flawil, Switzerland). The dried MS were weighed using a Mettler Toledo XS 105 dual range balance (Mettler Toledo Inc., Columbus, USA), and stored in a sealed or capped glass container at 4 °C for further analysis.

2.4. Microparticle characterization

2.4.1. Size, zeta potential and morphology

The size and size distribution of the EuSNa-TFV MS were evaluated using a Scepter 2.0 handheld, automated cell counter (Millipore, Billerica, MA, USA). The spray dried EuSNa-TFV MS were redispersed in deionized water at 1 mg/ml after 30 s sonication, and size was evaluated by Scepter using a 40 μm sensor (measuring range 3–13 μm). The zeta potential was measured at 25 °C using Zeta sizer (Zetasizer Nano ZS, Malvern Instruments Ltd, Worcestershire, UK). The surface characteristics and geometry of the MS were analyzed by scanning electron microscopy (SEM). For SEM analysis, a small amount of the powdered MS was put onto a grid. The membrane was mounted on a 1/2″ SEM stubs with double-sticky carbon tape. The sample was then sputter coated (Emitech EMS575SX) with ~20 nm thickness of gold and visualized under a Philips SEM 515 microscope (Philips/FEI, Eindhoven, NL).

2.4.2. Yield and powder flowability

The yield of the spray dried MS was simply calculated by the ratio of total mass of the spray dried powder to the total mass of the initial components combined. The powder flowability was measured by calculating Carr's index (Nekkanti et al., 2009). Briefly, the bulk density was measured by placing approximately one gram of powder under gravity into a calibrated graduated cylinder and then recording the bulk volume. The tapped density was measured by tapping the graduated cylinder on a wooden platform with an approximate amplitude of 20 mm until no further change in powder volume was observed (Chevanan et al., 2010; Ren et al., 2008). Carr's index was calculated through:

$$\text{Carrs index}(\%) = \frac{(\text{Tapped density} - \text{Bulk density})}{\text{Tapped density}} \times 100 \qquad (1)$$

2.4.3. Drug encapsulating efficiency

After spray drying, about 10 mg of EuSNa-TFV MS was dissolved using 5 ml of 95% alcohol at oscillation overnight. Five ml of water was then added into the solution. After vortexed for 1 min, the sample was analyzed using a RP-HPLC method at 259 nm (Agrahari and Youan, 2012). The HPLC system (Waters, Milford, MA) consisted of a 1575 binary pump system, 717 plus auto sampler, 2487 dual wavelength absorbance detector, and a Bridge™ C18 column (150 mm × 4.6 mm, 5 μm). The results were acquired and processed with Breeze™ software. The mobile phase was water (0.1% triethylamine, pH 5.1 adjusted by orthophosphoric acid) and acetonitrile (35:65 v/v) delivered at a flow rate of 1 mL/min. The standard curve was $y = 25.267x + 79.103$, $R^2 = 0.9994$. The drug encapsulation efficiency was calculated as:

$$\text{Drug encapsulation efficency}(\%) = \frac{\text{Actual loading}}{\text{Theoretical loading}} \times 100 \quad (2)$$

where actual loading was assessed by HPLC, and theoretical loading was calculated from the mass ratio between TFV and total mass of EuSNa-TFV MS.

2.4.4. In vitro release of TFV from EuSNa-TFV MS

To estimate the amount of TFV released from the MS, a protocol similar to the previously reported was used (Zhang et al., 2011). Two ml of resuspended EuSNa-TFV MS was put into a dialysis bag (Spectra/Por Float-A-Lyzer G2, MWCO 3.5-5 KD, Spectrum Laboratories Inc. Rancho Dominguze, CA, USA), and maintained in 40 ml of release medium using a shaking water bath (BS-06 Lab. Companion, Jeio Tech Co., LTD, Seoul, Korea) at 37 °C with an agitation speed of 60 rpm. Vaginal fluid simulant (VFS, pH 4.2) mixed with semen fluid simulant (VFS/SFS, pH 7.6) were used as a release medium (Owen and Katz, 1999, 2005). At predetermined time intervals (0, 0.25, 0.5, 1, 2, 3, 4 h) the amount of TFV released was measured by HPLC. Each sample was run in triplicate.

2.4.5. Powder X-ray diffraction analysis

Powder X-ray diffraction (XRD) analysis was performed on raw materials (S-100, TFV), blank EuSNa MS, two EuSNa-TFV MS formulations (high/low drug loading), and a physical mixture of EuSNa and TFV using the same ratio of dug vs. polymer. A MiniFlex automated X-ray diffractometer (Rigaku, The Woodland, Texas, USA) was used for the analysis at room temperature. The diffraction angle covered from 2 Θ 5° to 2 Θ 40°, and a step of 1° per min was applied. The diffraction patterns were processed using Jade 8+ (Materials Data, Inc., Livermore, CA).

2.5. Cell culture

Human vaginal epithelial cell line (VK2/E6E7, ATCC Number CRL-2616), Human Endocervical epithelial cell line (End1/E6E7, ATCC Number CRL-2615), and *Lactobacillus crispatus* (ATCC Number 33197) were obtained from the American Type Culture Collection (Manassas, VA, USA). Culture medium and reagents were purchased from Invitrogen (Carlsbad, CA, USA). VK2/E6E7 and End1/E6E7 cells were grown and routinely maintained at 37 °C in 75-cm^2 culture flasks, in keratinocyte-serum free medium supplemented with 0.1 ng/ml human recombinant EGF, 0.05 mg/ml bovine pituitary extract, additional calcium chloride 44.1 mg/L, and in an atmosphere of 5% CO_2.

2.6. Cell viability assay on vaginal/endocervical cell lines

The viability of VK2/E6E7 and End1/E6E7 cells was tested using both CellTiter 96™ Aqueous (MTS) and CellTiter 96™ Aqueous (LDH) assays (Promega, Madison, WI, USA) according to published protocol (Zhang et al., 2011). Cells were grown on a 96 well plate at 1×10^4 cells per well until they reached 80% confluence. Then the medium was changed and the cells were incubated with 100 μl of EuSNa-TFV MS at 1 mg/ml for 24 h. The medium was used as a negative control and 1% Triton X as a positive control. The plate was read using a DTX 800 multimode microplate reader (Beckman Coulter, Brea, CA, USA). Cell viability was calculated using the following Eq. (2) (for MTS assay) and 3 (for LDH assay):

$$Viability(\%) = \frac{ABS_{Test}}{ABS_{Control}} \times 100 \quad (3)$$

where ABS_{Test} and $ABS_{Control}$ represented the amount of formazan detected in viable cells.

$$Cytotoxicity(\%) = 100 \times \frac{Experimental - Background}{Positive - Background} \quad (4)$$

where experimental represent the fluorescence of MS-treated wells, background control wells contained cells not treated with MS, and positive control wells contained cells treated with 1% Triton X, respectively.

2.7. Lactobacillus viability assay

The viability of *L. crispatus* was evaluated using a MTS assay similar to the one described in the previous section. Briefly, *L. crispatus* was grown in an ATCC medium 416 Lactobacilli MRS broth (BD, Franklin Lakes, NJ, USA) at 37 °C and the bacteria population was adjusted to an OD_{670} of 0.06, which corresponds to a 0.5 McFarland Standard or 10^8 CFU/ml (Jorgenson et al., 1999). Then the bacterial was transferred to a 96 well plate and incubated with 100 μl of 1 mg/ml EuSNa-TFV MS for 24 h. Bacterial wells treated with commercially available Penicillin–Streptomycin solution (Invitrogen, Carlsbad, CA, USA) at 10 μg/ml were used as positive controls. The viability of *L. crispatus* was assessed using a CellTiter 96™ Aqueous kit and calculated according to Eq. (3).

2.8. In vitro cytokine release study

Cytokine levels were measured in VK and Endo cell culture supernatant by commercially available Milliplex MAP kits containing the human cytokine antibodies of IL-1α, IL-1β, IL-6, IL-8 and IP-10 (Millipore, Billerica, MA, USA). Similar cytokines have been found to be released by the same cell lines in previous toxicity studies with vaginal microbicidal products (Fichorova and Anderson, 1999; Fichorova et al., 2004). For this experiment, VK and Endo cell lines were grown on a 96 well plate until confluence, and then treated with 1 mg/ml EuSNa-TFV for 24 h in triplicate. Medium served as negative control and TNF-α at 50 ng/ml was used as positive control. The culture supernatant was collected and incubated with human cytokine antibodies at 4 °C overnight. The plate was analyzed using the Luminex 100 Multiplex system, and the cytokine concentrations were calculated by xPONENT V 3.1 software (Luminex Corp. Austin, TX, USA).

2.9. Preparation and characterization of oregon green conjugated EuSNa MS

Oregon green® 488 cadaverin *5-isomer* is an amine derivative of Oregon green® 488 dye, and it was used in this study to form OG conjugated EuSNa MS (EuSNa-OG MS). The synthesis scheme is shown in Fig. 1. It has been shown that this derivative can be successfully conjugated with a carboxyl group ended macromolecule, and maintain its fluorescence excitation and emission characteristics (Christie et al., 2009). Five hundred mg of Eudragit S-100 with

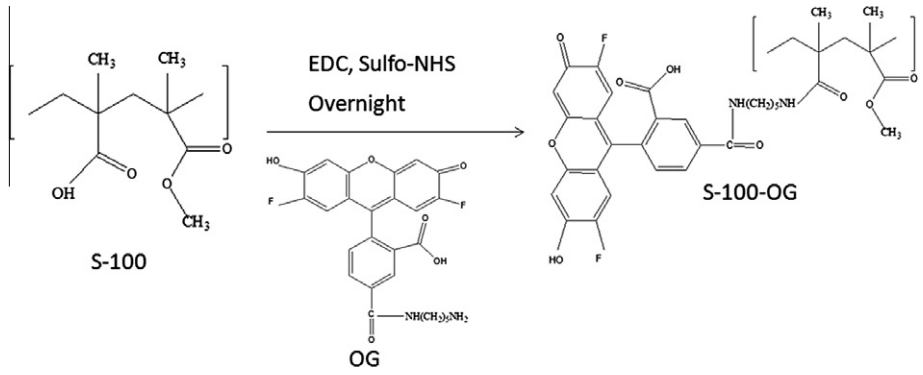

Fig. 1. Synthesis scheme of S-100 conjugated with Oregon green® 488 cadaverin *5-isomer* (OG), molecular weight 496.46.

Term	Estimate	Std Error	t Ratio	Prob>|t|
Polymer:drug ratio(10,40)	9.50875	1.781344	5.34	0.0129*
Polymer conc. (%, w/v)(2,5)	-7.51375	1.781344	-4.22	0.0244*
Feed flow rate (ml/min)(1.6,6.4)	4.39875	1.781344	2.47	0.0901
Polymer conc. (%, w/v)*Inlet temperature (°C)	-3.49375	1.781344	-1.96	0.1447
Polymer conc. (%, w/v)*Polymer:drug ratio	-3.35875	1.781344	-1.89	0.1558
Polymer conc. (%, w/v)*Feed flow rate (ml/min)	3.35125	1.781344	1.88	0.1565
Inlet temperature (°C)(100,140)	2.08375	1.781344	1.17	0.3266
Term	**Estimate**	**Std Error**	**t Ratio**	**Prob>|t|**
Polymer conc. (%, w/v)(2,5)	-6.3	0.584895	-10.77	0.0017*
Feed flow rate (ml/min)(1.6,6.4)	-3.925	0.584895	-6.71	0.0068*
Polymer conc. (%, w/v)*Polymer:drug ratio	-3.35	0.584895	-5.73	0.0106*
Inlet temperature (°C)(100,140)	3.075	0.584895	5.26	0.0134*
Polymer conc. (%, w/v)*Inlet temperature (°C)	-1.85	0.584895	-3.16	0.0508
Polymer conc. (%, w/v)*Feed flow rate (ml/min)	-0.35	0.584895	-0.60	0.5917
Polymer:drug ratio(10,40)	-0.175	0.584895	-0.30	0.7843
Term	**Estimate**	**Std Error**	**t Ratio**	**Prob>|t|**
Feed flow rate (ml/min)(1.6,6.4)	5.7	1.135797	5.02	0.0152*
Inlet temperature (°C)(100,140)	-5.665	1.135797	-4.99	0.0155*
Polymer conc. (%, w/v)*Inlet temperature (°C)	-3.4625	1.135797	-3.05	0.0555
Polymer conc. (%, w/v)*Polymer:drug ratio	-2.8025	1.135797	-2.47	0.0903
Polymer conc. (%, w/v)(2,5)	-2.0425	1.135797	-1.80	0.1700
Polymer:drug ratio(10,40)	0.915	1.135797	0.81	0.4794
Polymer conc. (%, w/v)*Feed flow rate (ml/min)	0.7825	1.135797	0.69	0.5404

Fig. 2. Pareto chart showing the standardized effect of independent variables and their interaction on Drug loading efficiency (top), Yield (middle) and Carr's Index (bottom). Bars extending past the line indicates statistical significance ($\alpha = 0.05$).

an average molecular weight of 125 KDa ($\sim 1.2 \times 10^{-7}$ M–COOH) was mixed using a magnetic stirrer with 11.5 mg EDC ($\sim 6 \times 10^{-6}$ M) and 33.5 mg sulfo-NHS ($\sim 1.5 \times 10^{-6}$ M) in phosphate buffer (pH 8.0 adjusted with NaOH) and maintained under room temperature for 20 min. OG (0.6 mg, 1:1 ratio of $-NH_2$ to –COOH) was added to the solution and the reaction was maintained for 24 h. The reaction mixture was then put into a dialysis bag (Spectra/Por Float-A-Lyzer G2, MWCO 3.5-5 KD, Spectrum Laboratories Inc. Rancho Dominguze, CA, USA) against 1000 ml of water for 24 h under magnetic stirring. The OG conjugated EuSNa was collected by lyophilization and further characterized using a Nicolet iS10 FT-IR Spectrometer (Thermo Scientific, West Palm Beach, FL) and ^{1}H 400 MHz NMR (Varian Inc., Santa Clara, CA, USA). The FT-IR spectrometer was equipped with a deuterated triglycine sulfate (DTGS) detector and controlled by OMNIC V 7.0 spectra software. The transmission mode in the FT-IR spectrometer was utilized to make observations with the sampling area of approximately 1 mm. Analysis was systematically performed between 650 and 4000 cm^{-1}. The background was collected at ambient conditions before analyzing each sample. Spectra was automatically corrected with a linear baseline. No specific sample preparation was used before the FT-IR analyses. For ^{1}H NMR analysis, all samples were dissolved in 100% D_2O. The data were recorded with 1024 scans, and the recycle time was set as 1 s at 25 °C. All data were analyzed by MestReNova LITE V 5.2.5-4731 software. The EuSNa-OG MS was prepared using the same method described in Section 2.3.

2.10. Mucoadhesion study

The scheme of the mucoadhesion test was adopted from published work, and some changes were made for this study (Nielsen et al., 1998). The study was performed on freshly obtained porcine vaginal tissue (Fairview Farm Meat Co., Topeka, KS, USA) within 2 h of death of the animal. The tissue was washed with normal saline, snap-frozen in liquid nitrogen, and kept at −80 °C. On the day of study, the tissue was first thawed at 4 °C, brought to room temperature gradually, and then cut into pieces of 8 cm length × 1 cm width. Cyanoacrylate glue previously used in a similar study (Meng et al., 2011) was applied to attach the tissue to a plastic strip, and then was inserted into a tube, which allowed the tissue to be mounted in a 37 °C water bath at an angle of 45°. An equilibration

Table 2
Response values of dependent variables.

Run no.	Pattern	Polymer Conc.(%, w/v)	Polymer: drug ratio	Inlet temperature (°C)	Feed rate (ml/min)	Drug encapsulation efficiency (%)	Yield (%)	Carr's index (%)
1	+−+−	5.0	10	140	1.6	45.7	64.3	16.7
2	−−+−	2.0	10	140	1.6	67.7	73.2	23.6
3	+−−+	5.0	10	100	6.4	64.0	53.3	47.9
4	−−−+	2.0	10	100	6.4	58.6	56.2	37.9
5	−+−−	2.0	40	100	1.6	82.3	69.7	35.5
6	++−−	5.0	40	100	1.6	60.8	54.8	31.2
7	++++	5.0	40	140	6.4	73.5	48.7	25.9
8	0	3.5	25	120	4.0	63.6	59.2	33.2
9	0	3.5	25	120	4.0	60.2	63.1	27.7
10	0	3.5	25	120	4.0	66.2	60.9	28.8
11	−+++	2.0	40	140	6.4	95.5	72.4	40.9

Table 3
The result of ANOVA and lack-of-fit analysis on all dependent variables.

Response	R^2	P_{ANOVA}	$P_{lack\text{-}of\text{-}fit}$
Drug encapsulation efficiency (Y_1)	0.95	0.047*	0.13
Yield (Y_2)	0.99	0.0077*	0.73
Carr's index (Y_3)	0.96	0.043*	0.32

* Statistical significance ($\alpha = 0.05$).

period of 5 min with VFS was allowed before administering the MS to humidify the mucosa. The mucosa was then continuously rinsed with 10 ml VFS (pre-equilibrated to 37 °C) containing fluorescent EuSNa-OG MS at 1 mg/ml. The flow rate was set at 1 ml/min using an infusion set. A 1% hydroxyethylcellulose gel, as well as a TFV loaded chitosan nanoparticle formulation (Meng et al., 2011), was used as control. The fluorescent intensities before and after the tissue rinsing were analyzed by a DTX 800 microplate reader at λ_{ex} 495 nm and λ_{em} 520 nm (Beckman Coulter, Brea, CA, USA). The percent of mucoadhesion was calculated as:

$$\text{Mucoadhesion}(\%) = \frac{F_1 - F}{F_1} \times 100 \quad (5)$$

where F_1 was the initial fluorescent intensity and F was the fluorescent intensity after the treatment.

After the study, the surface of the tissue was cleaned carefully and the tissue was cut into small cubes that were then embedded into Histoprep and frozen using liquid nitrogen. The vertical section from each frozen cube was mounted on a glass slide and examined with a Leica DMI3000 fluorescent microscope (Leica Microsystems GmbH, Wetzlar, Germany) using a total of 200X magnification.

2.11. Statistical analysis

The result of the 2^{4-1} design was analyzed using JMP software (version 8.0, SAS Institute Inc., Cary, NC, USA). Unless otherwise stated, data were expressed as mean ± standard deviations. Compared to controls, the statistical significant difference of a given mean was determined using a student's *t*-test. A P value < 0.05 was considered statistically significant.

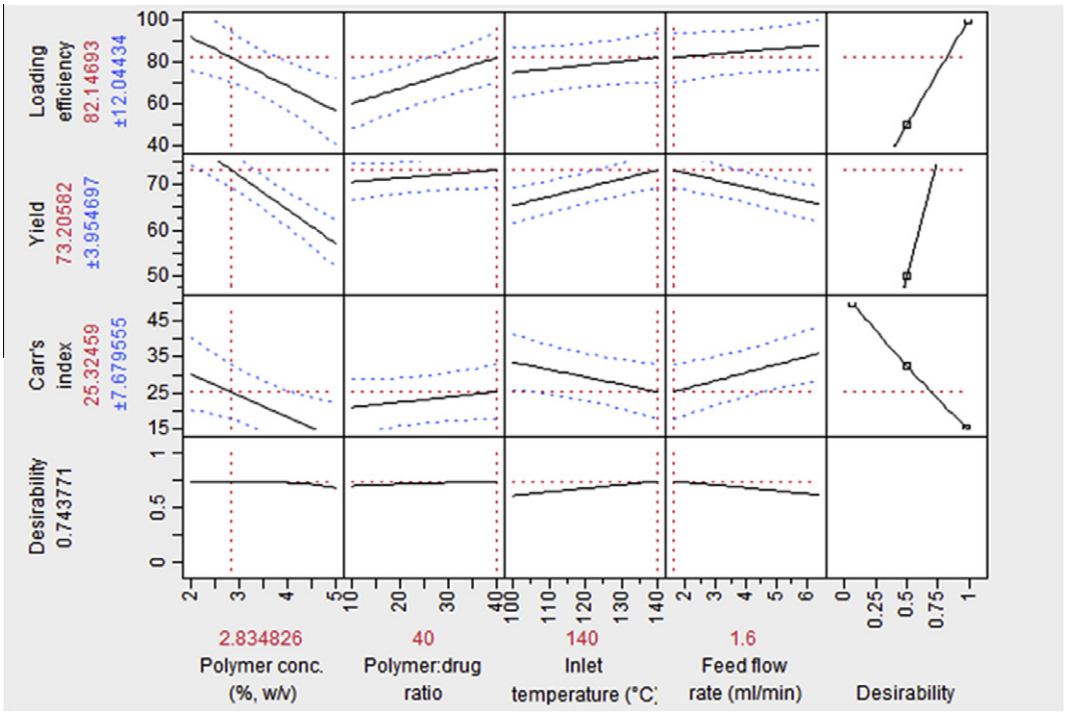

Fig. 3. Prediction and desirability plot showing the effect of independent variables on Drug loading efficiency, Yield, and Carr's index.

Table 4
Comparison between predicted and actual values of dependent variables under maximized desirability.

Run	Y_1 (%)	Predicted Y_1 (%)	*P*-value	Y_2 (%)	Predicted Y_2 (%)	*P*-value	Y_3 (%)	Predicted Y_3 (%)	*P*-value
OP*	88.7 ± 2.1	82.1 ± 12.0	0.40	68.9 ± 7.2	73.2 ± 3.9	0.41	28.3 ± 3.3	25.3 ± 7.67	0.56

* OP stands for optimum run.

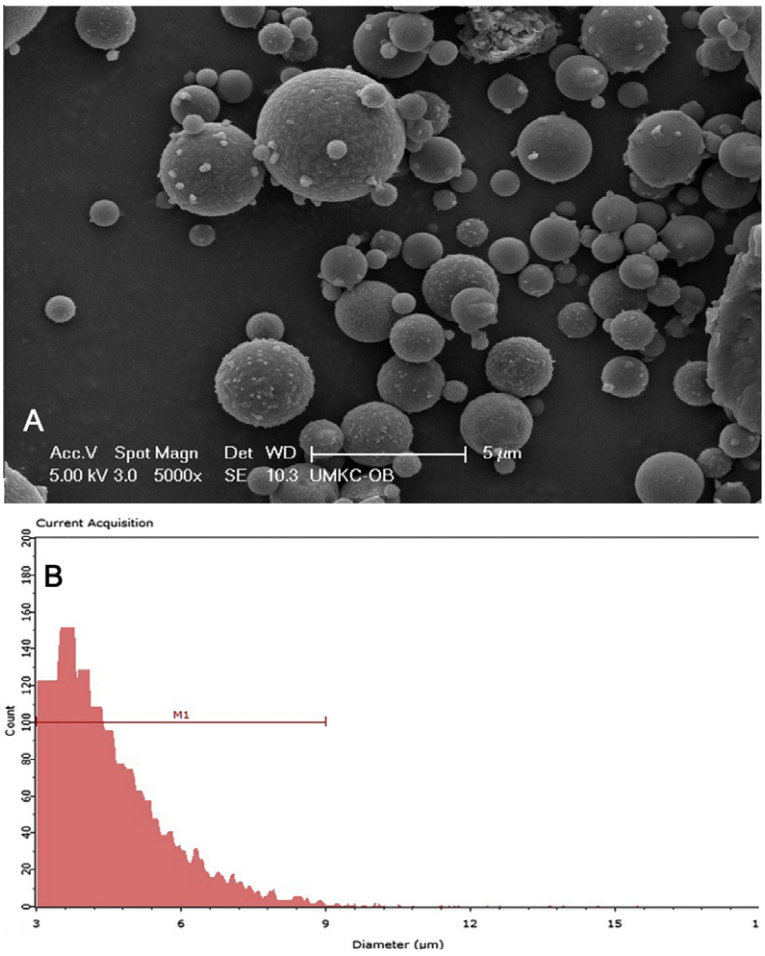

Fig. 4. (A) Scanning electron microscopy image of EuSNa-TFV MS. Scale bar set at 5 µm. (B) size distribution of EuSNa-TFV MS measured by Sceptor 2.0 cell counter. Y axis indicates the number of particle counts. M1 indicates a size region with lower limit of 3 µm and higher limit of 9 µm.

3. Results

3.1. Statistical analysis and optimization of EuSNa-TFV MS

Table 2 describes the responses obtained by the 2^{4-1} design for the drug encapsulation efficiency (Y_1), yield (Y_2) and Carr's index (Y_3). The overall drug encapsulation efficiency of EuSNa-TFV is greater than 50%, with a maximal encapsulation efficiency of 95.5%. The overall yield varies from 53% to 73%, with Carr's index ranging from 16.7 to 47.9. To check the validity of the model, ANOVA and lack-of-fit test were performed, and the results are shown in Table 3. All three dependent variables have R^2 values greater than 0.9. The *P* values for ANOVA are less than 0.05, indicating a statistically significant model fit at 95% confidence, with no lack-of-fit (*P* values for lack-of-fit test are greater than 0.05). Fig. 2 shows the main effect of all independent variables and their interactions on the dependent variables. The independent variables, which have an effect size (quantified by *t*-ratio) greater than a tabulated critical t value (t_{crit} = 3.18, df = 3, indicated by a blue vertical line), are identified as statistically significant. The overall effects of all the independent variables and their interactions are reflected by the following equations:

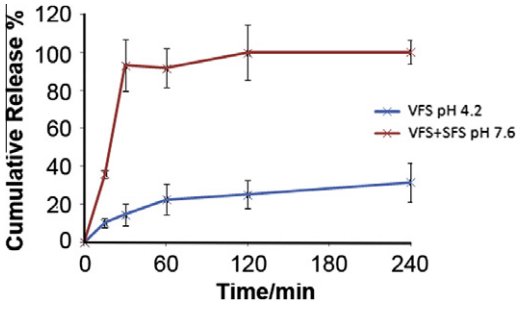

Fig. 5. *In vitro* release profile of EuSNa-TFV MS at pH = 4.2 (blue) and pH = 7.6 (red) under 37 °C, *n* = 3. (For interpretation of the references to colour in Fig. 2–10, the reader is referred to the web version of this article.)

Table 5
Kinetic models used for analysis of TFV loaded EuSNa MS release data and their corresponding R^2 values.

Model no.	Model name[a]	Model equation[b]	R^2 (pH 4.2)	R^2 (pH 7.6)
1	Zero order	$F = k_0 t$	0.759	0.983[c]
2	First order	$\ln(1-F) = -k_f t$	0.512	0.933
3	Higuchi	$F = k_H\sqrt{t}$	0.958	0.574
4	Power law	$\ln F = \ln k_p + p\ln t$	0.958	0.574
5	Weibull	$\ln[-\ln(1-F)] = \ln k_w + b\ln t$	0.964	0.862
6	Reciprocal powered time	$(1/F-1) = m/t^b$	0.969	0.544

[a] Models 1–5 were processed by linear regression where model 6 was processed by nonlinear regression.
[b] F denotes fraction of drug released at time t. k_0, k_f, k_H, k_p, p, k_w, b, and m are parameters of the models.
[c] Last three time points were not considered in the zero order model.

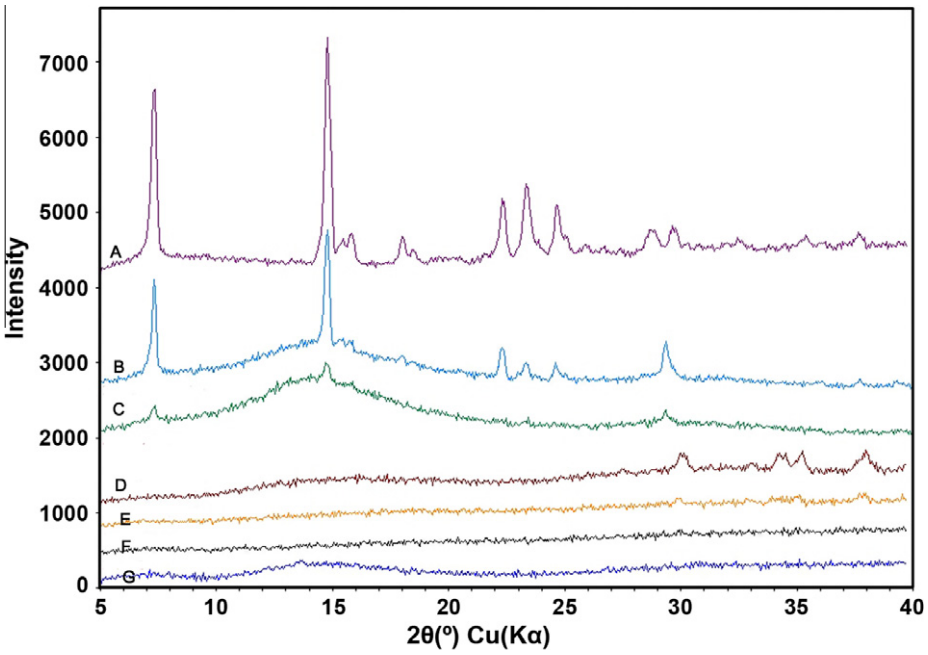

Fig. 6. XRD crystallography for drug loaded MS, raw component in the formulation and physical mixture of drug and polymer. From top to bottom, (A) pure TFV, (B) EuSNa and TFV mixture at 10:1, (C) EuSNa and TFV mixture at 40:1, (D) EuSNa-TFV MS (polymer to drug ratio 10:1), (E) EuSNa-TFV MS (polymer to drug ratio 40:1), (F) blank EuSNa MS, (G) pure Eudragit S-100.

$$Y_1 = 67.09 - 7.51X_{A1} + 9.51X_{A2} + 2.08X_{A3} + 4.39X_{A4} - 3.36X_{A1}X_{A2} - 3.49X_{A1}X_{A3} + 3.35X_{A1}X_{A4} \quad (6)$$

$$Y_2 = 61.44 - 6.3X_{A1} - 0.18X_{A2} + 3.07X_{A3} - 3.93X_{A4} - 3.35X_{A1}X_{A2} - 1.85X_{A1}X_{A3} - 0.35X_{A1}X_{A4} \quad (7)$$

$$Y_3 = 31.74 - 2.04X_{A1} + 0.92X_{A2} - 5.67X_{A3} + 5.7X_{A4} - 2.8X_{A1}X_{A2} - 3.46X_{A1}X_{A3} + 0.78X_{A1}X_{A4} \quad (8)$$

where the coded factors X_{Ai} are: $X_{A1} = (X_1-3.5)/1.5$, $X_{A2} = (X_2-25)/15$, $X_{A3} = (X_3-120)/20$ and $X_{A4} = (X_4-4)/2.4$, and X_1 through X_4 stand for the original independent variables in Table 1.

The relationship between the independent variables and dependent variables is further investigated using a prediction and desirability plot (Fig 3). In Fig. 3, the predicted values of all three dependent variables with their standard deviation values are represented by the solid line and the dotted line, respectively. Our goal was to maximize drug encapsulation efficiency (Y_1) and yield (Y_2) while minimize Carr's index (Y_3). Based on our goal, the optimum experimental condition is computed as: polymer concentration 2.8%, polymer to drug ratio 40:1, inlet temperature 140 °C, and feed flow rate of 1.6 ml/min, with a maximized desirability value of 0.74. The comparison between the predicted and the actual values of the dependent variables is achieved by a check point analysis shown in Table 4. The differences between the predicted and actual values appear to be statistically insignificant.

3.2. Size, zeta potential and morphology of EuSNa-TFV MS

As shown in Fig. 4A, TFV loaded EuSNa MS appear to be well dispersed and spherical in shape. There is a variance in size distribution as shown in Fig. 4B; however, most particles appear to be greater than 2 μm. The average size of spray dried EuSNa-TFV MS is 4.73 μm as measured by a Scepter 2.0 handheld automated cell counter. The average zeta potential of EuSNa-TFV-MS is −26.3 mV.

3.3. In vitro release of tenofovir from EuSNa-TFV MS

The *in vitro* release profile of TFV loaded EuSNa MS in VFS and a mixture of VFS/SFS is shown in Fig. 5. There is 91.7 ± 10.7% ($n = 3$) of TFV released from EuSNa MS at pH 7.6 within 60 min, while there's only 22.5 ± 8.1% ($n = 3$) of TFV released at pH 4.2 during the same period of time. The simulation of the release profile of TFV to a series of known release kinetic models is performed and the results are shown in Table 5. The release of TFV from the MS at pH 7.6 appears to follow zero-order kinetics, while the release

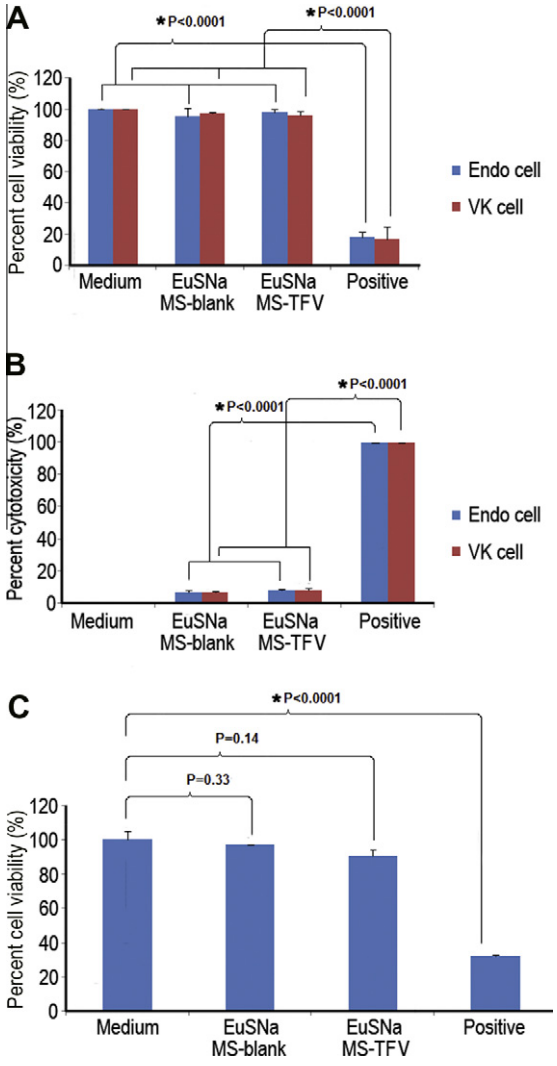

Fig. 7. MTS (A) and LDH (B) assay of VK and Endo cells treated with blank or TFV loaded EuSNa MS at 1 mg/ml over 24 h. (C) Viability of Lactobacillus cripatus treated with blank or EuSNa TFV-loaded MS after 24 h at 1 mg/ml. The data shown represent the mean ± standard deviation of 3 independent experiments. *Statistical significance ($\alpha = 0.05$).

profile under pH 4.2 can be better described by reciprocal powered time model.

3.4. X-ray diffraction analysis

The result of X-ray diffraction analysis is shown in Fig. 6. The characteristic peaks of TFV are found around $2\theta = 7°$, 15°, 22°, 23.5° and 24.8°. These peaks are not observed in any of the EuSNa MS formulations, while they are still observable in the physical mixture of TFV and EuSNa using the same mass ratio.

3.5. Cytotoxicity study of EuSNa-TFV MS

Our data suggest that EuSNa-TFV MS is safe in both vaginal (VK) and endocervical (Endo) epithelial cell lines (Fig. 7). No significant reduction of cell viability was found in MTS assay (Fig. 7A) using both blank and drug loaded MS formulation at 1 mg/ml. Lactate dehydrogenase (LDH) is an indicator released from cells with damaged membranes. Minimal amount of LDH was released from cells incubated with blank and drug loaded EuSNa MS, being only 6.9% and 7.7% compared to positive control, respectively (Fig. 7B). The result also indicates that EuSNa-TFV MS is not toxic to vaginal flora, as no statistically significant loss of viability was found during the incubation period (Fig. 7C).

3.6. Cytokine release study

The level of immunogenicity of EuSNa-TFV MS is evaluated using the Luminex Multiplex system and the results are shown in Fig. 8. The concentration of five cytokines, namely IL-1α, IL-1β, IL-6, IL-8, and IP-10 are shown after 24 h incubation with EuSNa-TFV MS. In case of IL-6, IL-8, and IP-10, the level of cytokine released is comparable, or even lower, than that of the medium (Fig. 8A–C), while significantly lower than the positive control (TNF-α at 50 ng/ml). A similar trend can be observed in cases of IL-1α and IL-1β; however, IL1-α and IL1-β are not able to generate similar level of cytokine as they did in IL-6, 8 and IP-10.

3.7. Mucoadhesion study

Fig. 9A shows the FT-IR spectrum of S-100 polymer, EDC, Sulfo-NHS (S-NHS), and S100-OG conjugate. The C=O stretching vibration signal around 1700 cm^{-1} is reduced and substituted with a peak of similar strength around 1600 cm^{-1}, which is due to the formation of an amide bond (Gallagher, 2011). The broad peak around 3300 to 3500 cm^{-1} may be contributed to NH stretching vibrations. In Fig. 9B, the existence of Oregon green in S100-OG conjugate is proved by ^1H NMR spectroscopy. The aromatic proton peaks (δ = 8.20, 8.05, 7.81, 7.24, 6.69 and 6.58) can be detected in the final product S100-OG, and the line width of the peaks at the aromatic areas is consistent with dye bonding with polymer. In Fig. 10A, OG conjugated EuSNa MS can be observed with a strong fluorescent signal.

The mucoadhesion of EuSNa MS was evaluated and the results are shown in Fig. 10B–D. The average mucoadhesion of EuSNa MS is determined to be 8.7%, where mucoadhesion of HEC gel and chitosan nanoparticles is 4.4% and 8.1%, respectively. The mucoadhesion of EuSNa is found to be slightly higher that of chitosan nanoparticles, and it is significantly greater than that of 1% HEC gel formulation.

4. Discussion

The purpose of the 2^{4-1} fractional factorial design is to screen several key factors contributing to the optimum formulation with high-yield, high drug encapsulation efficiency, and low moisture content during the formulation design and process. For drug encapsulation efficiency (Y_1), it is found that increasing the polymer to drug ratio, as well as decreasing polymer concentration, can significantly improve drug encapsulation. High drug encapsulation efficiency can be achieved through high polymer to drug ratio, indicating the possibility that the free drug, which is not associated with the polymer, is less likely to be well encapsulated. It is not clear as of how decreasing polymer concentration contributes to high encapsulation efficiency. For yield (Y_2), it is found that low polymer concentration, low feed flow rate, and high inlet temperature are capable of significantly improving the yield of the spray dried MS. The effect of inlet temperature and feed flow rate on spray drying is shown in the following equation (Hamdy et al., 2011; Hung et al., 2011):

$$\eta_{overall} = \left(\frac{T_1 - T_2}{T_1 - T_0}\right) \times 100 \quad (9)$$

where $\eta_{overall}$ denotes the overall thermal efficiency, T_1 is inlet temperature, T_2 is outlet temperature, and T_0 is the atmospheric temperature. Therefore by increasing inlet temperature (T_1), the

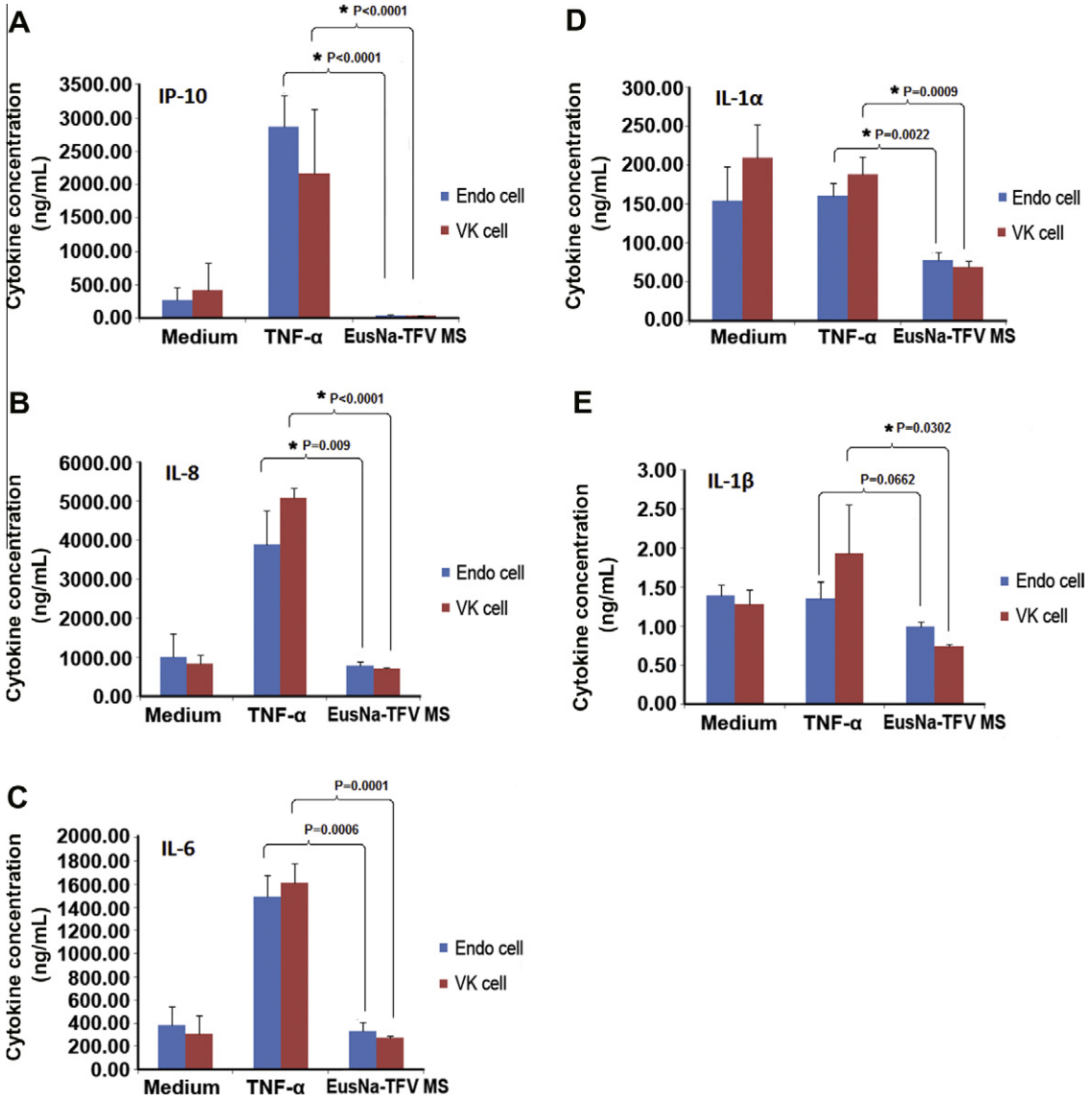

Fig. 8. The level of cytokine release from VK and Endo cells treated with TFV-loaded EuSNa MS over 24 h. (A) IP-10, (B) IL-8, (C) IL-6, (D) IL-1α, (E) IL-1β. The data shown represent the mean ± standard deviation of 3 independent experiments. *Statistical significance (α = 0.05).

overall thermal efficiency is increased, leading to better drying and higher yield.

$$n_{a/f} = \frac{V_{aa} \times \rho_a}{V_{lf} \times \rho_f} \tag{10}$$

where the relationship between the liquid feeding rate (V_{lf}), the atomizing air flow rate (V_{aa}), and their influence on spray drying, was defined by the air/fluid mass ratio ($n_{a/f}$). The so-called air/fluid mass ratio represents the energy available for atomization, and decreasing $n_{a/f}$ will result in insufficient drying of particles (Patterson et al., 2005). When atomizing air flow is fixed, decreasing liquid feeding rate increases $n_{a/f}$, therefore increasing drying efficiency leads to increased yield. The Carr's index (Y_3) is an indicator of the powder flowability of the spray dried powder. The value of Carr's index, which is greater than 25%, indicates a cohesive powder with poor flow characteristics (Gonnissen et al., 2008). Increased feed flow rate, as well as low temperature, is found to have a significant effect on increasing Carr's index. In practice, poor powder flowability is usually correlated with high moisture residue in the powder, which can be an obvious consequence from increased feed flow rate and low temperature as the combination suffers from insufficient drying.

The concept of maximized desirability was used in this study to find the optimum condition. The desirability in optimization of multiple dependent variables is described using a scale of 0 to 1, where 0 is not acceptable and 1 is the perfectly desirable result (Derringer and Suich, 1980). The optimum formulation has an average encapsulation efficiency of 88.7% with 68.9% yield, and a Carr's index of 28.3%. The surface characteristics of the particulate system usually govern its biological fate, especially if delivered topically. In terms of intravaginal delivery, the mucus serves as a barrier that can filter out particles with a large size (>1 μm), rendering these particles only adhering on the mucus surface (das Neves et al., 2011). Smaller particles may be more capable of diffusing through the mucin mesh, which has been experimentally confirmed that a suitable size range (200–500 nm) is required for muco-penetration (Ham et al., 2009). However, in this study, the EuSNa-TFV MS was designed to be responsive to the pH change caused by male ejaculate. Therefore a mucin-adhering, rather than

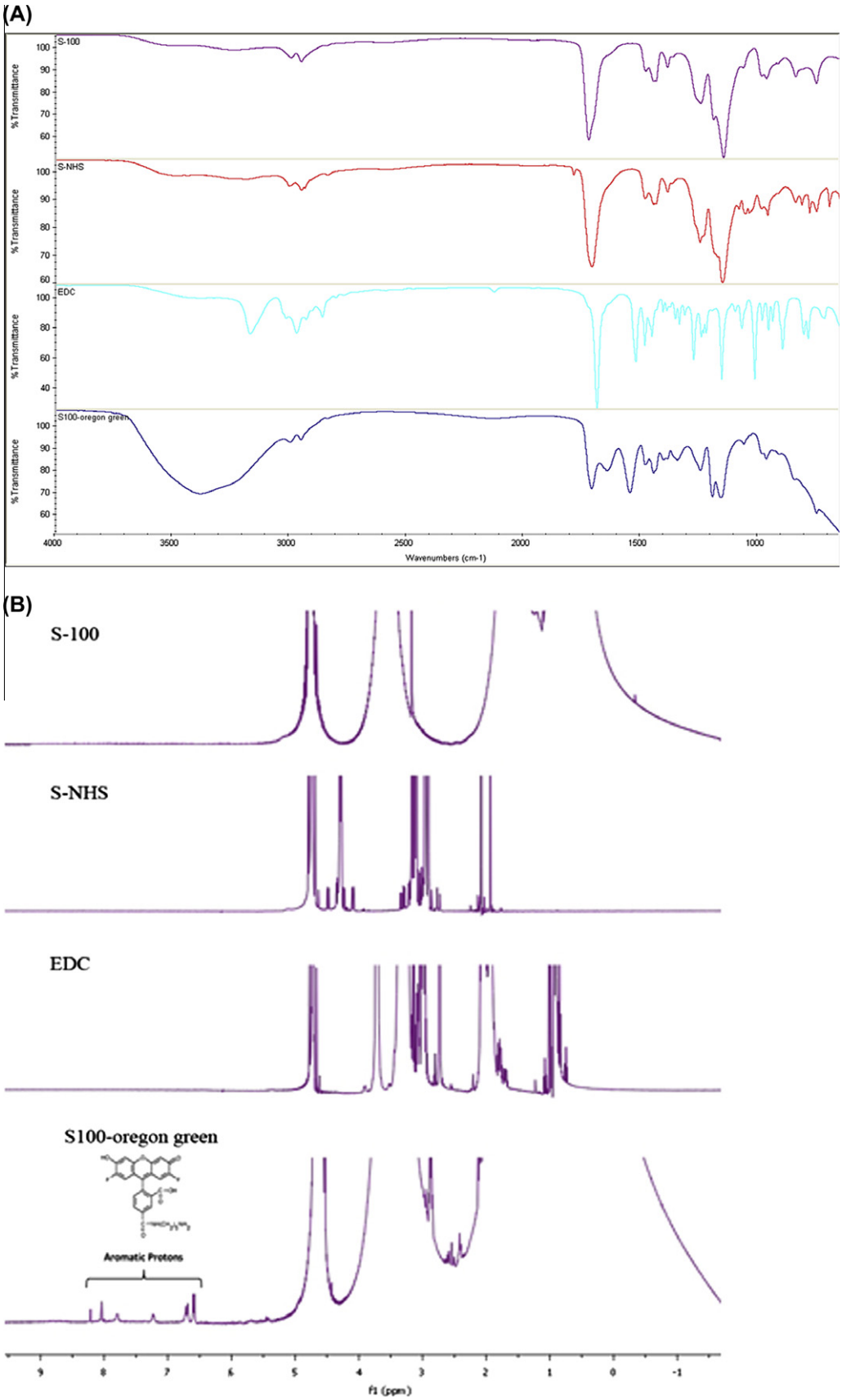

Fig. 9. (A) FT-IR spectrum of the reactants and the product of EuSNa-OG complex. From top to bottom: FT-IR spectrum of pure S-100, Sulfo-NHS, EDC, EuSNa-OG conjugate. (B) NMR spectrum showing the aromatic protons in the EuSNa-OG complex.

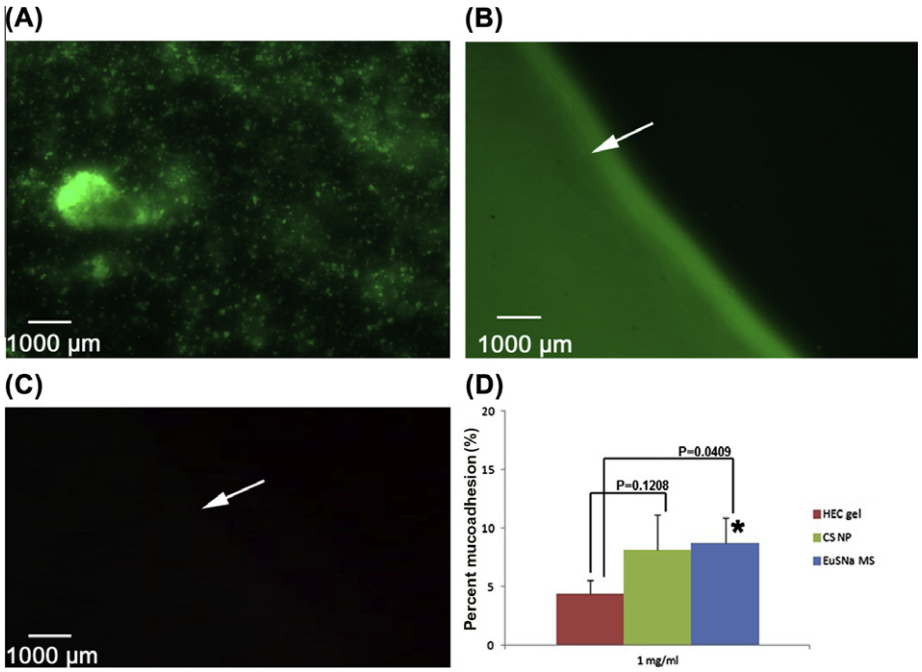

Fig. 10. (A) Fluorescent microscopy image of Oregon green loaded MS. (B) Vertical section of porcine vaginal tissue after the mucoadhesion study, arrow showing the surface of the vaginal tissue section. (C) Control fluorescent image of the same porcine vaginal tissue represented in figure B, arrow showing the same position as in figure B. (D) Percentage mucoadhesion of 1 mg/ml HEC gel, chitosan nanoparticles and EuSNa MS. *Statistical significance ($\alpha = 0.05$).

a mucin-penetrating, delivery system may better serve this purpose. Surface charge serves as another important characteristic that determines whether a particle delivery system will penetrate through the mucin. For example, it has been found that small particles with neutral surface charge have a better chance at reaching deep into the epithelium (Wang et al., 2008). Therefore the relatively large size, combined with strong surface charge, of EuSNa-TFV MS may guarantee that it could be in the right place as a pH-sensitive delivery micro system.

TFV is a hydrophilic molecule (Log$P$ −1.6) with a molecular weight of 287.12. It's very difficult to achieve high TFV loading using a nanoparticle delivery system prepared by the traditional emulsion-evaporation method (Zhang et al., 2011), in which hydrophilic drug like TFV is very likely present in the aqueous phase and therefore being washed out during the preparation process. In this study, the average drug loading of TFV is 2% (w/w), which means that a 1 mg/ml EuSNa-TFV MS suspension is equivalent to a TFV concentration of 69.7 μM. This is almost 10 times higher than the TFV loading in the pH-sensitive nanoparticles prepared by the emulsion-evaporation technique (Zhang et al., 2011).Given the fact that the EC_{50} of TFV is 5.0 ± 2.6 μM, it is reasonably speculated that this MS formulation can provide a sufficient concentration of TFV to exhibit an anti-HIV effect after complete drug release within 2 h following the vaginal pH change tiggerred by the seminal fluid (Lee et al., 2005). Spray drying as a quick and easy preparation method, not only produces large and spherical particles that have a good impact on powder flowability (Hamdy et al., 2011), but also changes the TFV from its crystallized form. As seen in Fig. 6, the characteristic peaks of TFV are still observable in the physical mixture of TFV with EuSNa, but almost completely lost in the crystallography of spray dried MS formulations, suggesting that TFV appears to be amorphous in the MS formulation. It has been shown in the previous studies that TFV could exist in either crystalline or amorphous form in the formulation using different process (Johnson et al., 2010; Zidan et al., 2010). However, it is known that compounds in crystalline form often display higher stability yet lower aqueous solubility as well as bioavailability (Newman and Byrn, 2003). Our stability study indicates that TFV is stable under acidic pH (data not shown). However, comparative study on the stability of both crystalline and amorphous TFV within the MS remained to be performed. Since the altered pH inside the vagina can be maintained for only a couple of hours after ejaculate (Tevi-Benissan et al., 1997), it is critical that any pH-sensitive delivery system has a fast release rate at alkaline pH. The EuSNa-TFV MS can release almost 90% of its pay load within 60 min at pH 7.6, while only approximately 20% of the TFV is released in the same period at the acidic pH condition of the normal vagina. The portion of drug released at an acidic pH may be due to the surface-associated or free TFV present in the formulation. It is well known that S100 is dissolved when the pH is above 7 (Degussa, 2011). Although the vaginal pH may vary among healthy women, it is reported that the range of normal vaginal pH is between 4.1 to 6.0 (Stevens-Simon et al., 1994). Bacteria vaginosis as well as other STI may cause the vaginal pH to be above 6, but in this case a pretreatment or pH-buffering agent may be administered before applying the formulation in clinical setting. The TFV release from EuSNa-TFV MS under pH 7.6 appears to follow zero order release kinetic within the first 60 min, while its release under pH 4.2 would be best fit by a reciprocal powered (RP) model. It is possible that under alkaline pH, the fast dissolution of Eudragit S-100 will make the MS a porous matrix; and it has been shown that small molecules released from porous polymer microcarriers are likely to follow zero-order release (Jankower and Shipley, 1989). In the RP model, not only dissolution and diffusion, but also other time dependent variables, are embedded into the model (Mohammadi et al., 2010), such as wettability and degradation of S-100 in this case.

Safety is also an important factor in developing a topical delivery system, as it has been pointed out that a safe microbicide delivery system cannot damage the vaginal/endocervical epithelium, disturb normal vaginal flora, or trigger any immune-response (Team, 2010). In this study, MTS and LDH assay show that 1 mg/ml

EuSNa-TFV MS is safe to both vaginal and endocervical epithelium with no significant reduction of viability. The normal vaginal flora will not be affected, either. Fig. 8 shows the level of inflammatory cytokine release on VK and Endo cell lines. These cytokines are chosen because of their extensive involvement in mucosa toxicity research both *in vitro* and *in vivo* (Fichorova et al., 2004, 2005; Genc et al., 2004). In case of IL-6, IL-8 and IP-10, the level of cytokine triggered by EuSNa-TFV MS is significantly lower compared to the positive control, suggesting its immunogenicity is transient. In case of IL-1α, the overall level of cytokine release is low, suggesting the cells may not be sensitive enough for both TNF-α and EuSNa-TFV MS. However, the level of IL-1α is still significantly lower than TNF-α. The total level of cytokine is even lower in case of IL-1β. This might suggest that IL-1α and β are not suitable cytokines to be tested *in vitro* on these two cell lines. As in some studies a good correlation between the rabbit vaginal irritation scores and IL-1β levels in vagina lavage has been shown (Fichorova et al., 2004), suggesting it might be better detected in future *in vivo* test. However, overall there is no evidence of significant cytokine release triggered by EuSNa-TFV MS in this study.

During the synthesis of EuSNa-OG complex, the dialysis method was applied overnight to ensure the removal of any free OG molecule. As is shown in the FT-IR and NMR spectrum, both amide bond stretch and aromatic protons can be observed in the final synthetically fluorescent MS, which indicates the successful conjugation of OG to the polymethacrylate. These facts together prove that the OG has been successfully covalently attached to EuSNa MS and the fluorescent signal in mucoadhesion study is not due to free OG.

Porcine vaginal tissue was used in this study as it provides a physiologically relevant and sensitive system that can be utilized in *ex vivo* scenario (D'Cruz et al., 2005). It has been reported that the Eudragit salts have a high intrinsic dissolution rate and the dissolved chain could interact strongly with the hydrated mucin glycoprotein (Cilurzo et al., 2003, 2005). The *in vitro* mucoadhesion test indeed demonstrates a statistically significant improvement in term of mucoadhesion of EuSNa MS compared to HEC gel (Fig. 10D). This percent mucoadhesion is slightly higher than that of chitosan nanoparticle formulation under the similar experimental condition (Meng et al., 2011). Our hypothesis in this study is to incorporate a mucoadhesive material to our delivery system, and by doing so prolong the bioretention time of such system. Therefore, when the triggering stimuli is present (semen in this case), it is anticipated that the drug will undergo immediate release at high concentration.

5. Conclusion

In this study, spray dried, tenofovir loaded, pH sensitive, and mucoadhesive microspheres are prepared based on polymethacrylate salt. Fractional factorial design has been used to screen and optimize formulation and process parameters. The optimized formulation has an average size of 4.73 μm with an drug loading of 2% (w/w). It has been shown that these microspheres can quickly respond to the pH change, releasing over 90% of drug payload within 60 min. The mucoadhesion property of these microspheres is significantly improved compared to 1% HEC gel formulation. Moreover, the findings in this study reveal that these microspheres are non-cytotoxic and non-immunogenic to vaginal/endocervical epithelial cells. There is also no observable cytotoxic effect on normal vaginal flora. These microspheres are potentially more effective for intravaginal delivery of microbicides, owing to their improved mucoadhesion and pH-responsiveness. Future studies are needed to evaluate their vaginal retention and safety *in vivo*. Collectively, these data present a possible delivery strategy for intravaginal delivery of microbicides for the prevention of HIV transmission.

6. Glossary

[3-(4,5-dimethylthiazol-2-yl)-5-(3-carboxymethoxyphenyl)-2-(4-sulfophenyl)-2H-tetrazolium] solution: MTS, Dynamic light scattering: DLS, Eudragit S-100: S-100, Eudragit S-100 sodium salt (EuSNa), Lactate dehydrogenase: LDH, Microparticles: (MS), Nanoparticles: NP, Oregon green: OG, Powder X-ray diffraction: (XRD), Pre-exposure prophylaxis: PrEP, Scanning electron microscopy: SEM, Semen fluid simulant: SFS, Tenofovir: TFV, Vaginal fluid simulant: VFS.

Acknowledgements

The work presented was supported by Award Number R01AI087304 from the National Institute of Allergy And Infectious Diseases. The content is solely the responsibility of the authors and does not necessarily represent the official views of the National Institute of Allergy And Infectious Diseases or the National Institutes of Health. The authors would like to thank Dr. Vladimir Dusevich (Director, Electron Microscopy Facility, School of Dentistry, University of Missouri-Kansas City, MO) for the electron microscopy, and Fairview Farm Meat Co. (Topeka, KS) for providing the porcine vaginal tissue.

References

Agrahari, V., Youan, B.B., 2012. Sensitive and rapid HPLC quantification of tenofovir from hyaluronic acid-based nanomedicine. AAPS PharmSciTech 13, 202–210.
Chevanan, N., Womac, A.R., Bitra, V.S., Igathinathane, C., Yang, Y.T., Miu, P.I., Sokhansanj, S., 2010. Bulk density and compaction behavior of knife mill chopped switchgrass, wheat straw, and corn stover. Bioresour. Technol. 101, 207–214.
Christie, R.J., Tadiello, C.J., Chamberlain, L.M., Grainger, D.W., 2009. Optical properties and application of a reactive and bioreducible thiol-containing tetramethylrhodamine dimer. Bioconjug. Chem. 20, 476–480.
Cilurzo, F., Minghetti, P., Selmin, F., Casiraghi, A., Montanari, L., 2003. Polymethacrylate salts as new low-swellable mucoadhesive materials. J. Control. Release 88, 43–53.
Cilurzo, F., Selmin, F., Minghetti, P., Rimoldi, I., Demartin, F., Montanari, L., 2005. Fast-dissolving mucoadhesive microparticulate delivery system containing piroxicam. Eur. J. Pharm. Sci. 24, 355–361.
Clark, M.R., Aliyar, H.A., Lee, C.W., Jay, J.I., Gupta, K.M., Watson, K.M., Stewart, R.J., Buckheit, R.W., Kiser, P.F., 2011. Enzymatic triggered release of an HIV-1 entry inhibitor from prostate specific antigen degradable microparticles. Int J Pharm 413, 10–18.
das Neves, J., Michiels, J., Arien, K.K., Vanham, G., Amiji, M., Bahia, M.F., Sarmento, B., 2011. Polymeric nanoparticles affect the intracellular delivery, antiretroviral activity and cytotoxicity of the microbicide drug candidate dapivirine. Pharm. Res. 2012, 1468–1484.
D'Cruz, O.J., Erbeck, D., Uckun, F.M., 2005. A study of the potential of the pig as a model for the vaginal irritancy of benzalkonium chloride in comparison to the nonirritant microbicide PHI-443 and the spermicide vanadocene dithiocarbamate. Toxicol. Pathol. 33, 465–476.
Degussa, 2011. EUDRAGIT L 100® and EUDRAGIT S 100 ® Specification and Test Methods.
Derringer, G., Suich, R., 1980. Simutaneous optimization of several response variables. J. Qual. Technol. 12, 214.
FHI, 2011. VOICE HIV Prevention Trial Discontinues Tenofovir Gel Arm for Futility.
Fichorova, R.N., Anderson, D.J., 1999. Differential expression of immunobiological mediators by immortalized human cervical and vaginal epithelial cells. Biol. Reprod. 60, 508–514.
Fichorova, R.N., Bajpai, M., Chandra, N., Hsiu, J.G., Spangler, M., Ratnam, V., Doncel, G.F., 2004. Interleukin (IL)-1, IL-6, and IL-8 predict mucosal toxicity of vaginal microbicidal contraceptives. Biol. Reprod. 71, 761–769.
Fichorova, R.N., Zhou, F., Ratnam, V., Atanassova, V., Jiang, S., Strick, N., Neurath, A.R., 2005. Anti-human immunodeficiency virus type 1 microbicide cellulose acetate 1,2-benzenedicarboxylate in a human *in vitro* model of vaginal inflammation. Antimicrob. Agents Chemother. 49, 323–335.
Gallagher, W., 2011. FTIR Analysis of Protein Structure. Available from: <http://www.chem.uwec.edu/chem455_S05/Pages/Manuals/FTIR_of_proteins.pdf>. (Accessed on 12/09/2011).
Garg, S., Goldman, D., Krumme, M., Rohan, L.C., Smoot, S., Friend, D.R., 2010. Advances in development, scale-up and manufacturing of microbicide gels, films, and tablets. Antiviral Res. 88 (Suppl 1), S19–S29.
Genc, M.R., Vardhana, S., Delaney, M.L., Onderdonk, A., Tuomala, R., Norwitz, E., Witkin, S.S., 2004. Relationship between a toll-like receptor-4 gene polymorphism, bacterial vaginosis-related flora and vaginal cytokine

responses in pregnant women. Eur. J. Obstet. Gynecol. Reprod. Biol. 116, 152–156.
Gonnissen, Y., Remon, J.P., Vervaet, C., 2008. Effect of maltodextrin and superdisintegrant in directly compressible powder mixtures prepared via co-spray drying. Eur. J. Pharm. Biopharm. 68, 277–282.
Gupta, K.M., Barnes, S.R., Tangaro, R.A., Roberts, M.C., Owen, D.H., Katz, D.F., Kiser, P.F., 2007. Temperature and pH sensitive hydrogels: an approach towards smart semen-triggered vaginal microbicidal vehicles. J. Pharm. Sci. 96, 670–681.
Ham, A.S., Cost, M.R., Sassi, A.B., Dezzutti, C.S., Rohan, L.C., 2009. Targeted delivery of PSC-RANTES for HIV-1 prevention using biodegradable nanoparticles. Pharm. Res. 26, 502–511.
Hamdy, S., Haddadi, A., Ghotbi, Z., Hung, R.W., Lavasanifar, A., 2011. Part I: targeted particles for cancer immunotherapy. Curr. Drug Deliv. 8, 261–273.
Hung, R.W., Hamdy, S., Haddadi, A., Ghotbi, Z., Lavasanifar, A., 2011. Part II: targeted particles for imaging of anticancer immune responses. Curr. Drug Deliv. 8, 274–281.
Jankower, L., Shipley, W., 1989. Controlled Release Formulating Employing Resilient Microbeads. US.
Johnson, T.J., Gupta, K.M., Fabian, J., Albright, T.H., Kiser, P.F., 2010. Segmented polyurethane intravaginal rings for the sustained combined delivery of antiretroviral agents dapivirine and tenofovir. Eur. J. Pharm. Sci. 39, 203–212.
Jorgenson, J.H., Turnidge, J.D., Washington, J.A., 1999. Antibacterial susceptibility tests: dilution and disk diffusion methods. In: Murray, P.R., Baron, E.J., Pfaller, M.A., Tenover, F.C., Yolken, R.H. (Eds.), Manual of clinical microbiology, 7 ed. ASM Press, Washington DC.
Karim, Q.A., Karim, S.S., Frohlich, J.A., Grobler, A.C., Baxter, C., Mansoor, L.E., Kharsany, A.B., Sibeko, S., Mlisana, K.P., Omar, Z., Gengiah, T.N., Maarschalk, S., Arulappan, N., Mlotshwa, M., Morris, L., Taylor, D., 2010. Effectiveness and safety of tenofovir gel an antiretroviral microbicide for the prevention of HIV infection in women. Science 329 (5996), 1168–1174.
Lee, W.A., He, G.X., Eisenberg, E., Cihlar, T., Swaminathan, S., Mulato, A., Cundy, K.C., 2005. Selective intracellular activation of a novel prodrug of the human immunodeficiency virus reverse transcriptase inhibitor tenofovir leads to preferential distribution and accumulation in lymphatic tissue. Antimicrob. Agents Chemother. 49, 1898–1906.
Mahalingam, A., Jay, J.I., Langheinrich, K., Shukair, S., McRaven, M.D., Rohan, L.C., Herold, B.C., Hope, T.J., Kiser, P.F., 2011. Inhibition of the transport of HIV *in vitro* using a pH-responsive synthetic mucin-like polymer system. Biomaterials 32, 8343–8355.
Mbopi-Keou, F.X., Trottier, S., Omar, R.F., Nkele, N.N., Fokoua, S., Mbu, E.R., Domingo, M.C., Giguere, J.F., Piret, J., Mwatha, A., Masse, B., Bergeron, M.G., 2010. A randomized, double-blind, placebo-controlled phase II extended safety study of two invisible condom formulations in cameroonian women. Contraception 81, 79–85.
McCormack, S., Ramjee, G., Kamali, A., Rees, H., Crook, A.M., Gafos, M., Jentsch, U., Pool, R., Chisembele, M., Kapiga, S., Mutemwa, R., Vallely, A., Palanee, T., Sookrajh, Y., Lacey, C.J., Darbyshire, J., Grosskurth, H., Profy, A., Nunn, A., Hayes, R., Weber, J., 2010. PRO2000 vaginal gel for prevention of HIV-1 infection (Microbicides Development Programme 301): a phase 3, randomised, double-blind, parallel-group trial. Lancet 376, 1329–1337.
Meng, J., Sturgis, T.F., Youan, B.B., 2011. Engineering tenofovir loaded chitosan nanoparticles to maximize microbicide mucoadhesion. Eur. J. Pharm. Sci. 44, 57–67.
Mohammadi, G., Barzegar-Jalali, M., Valizadeh, H., Nazemiyeh, H., Barzegar-Jalali, A., Siahi Shadbad, M.R., Adibkia, K., Zare, M., 2010. Reciprocal powered time model for release kinetic analysis of ibuprofen solid dispersions in oleaster powder, microcrystalline cellulose and crospovidone. J. Pharm. Pharm. Sci. 13, 152–161.
Morrow, K.M., Ruiz, M.S., 2008. Assessing microbicide acceptability: a comprehensive and integrated approach. AIDS Behav. 12, 272–283.
Nekkanti, V., Muniyappan, T., Karatgi, P., Hari, M.S., Marella, S., Pillai, R., 2009. Spray-drying process optimization for manufacture of drug-cyclodextrin complex powder using design of experiments. Drug Dev. Ind. Pharm. 35, 1219–1229.
Newman, A.W., Byrn, S.R., 2003. Solid-state analysis of the active pharmaceutical ingredient in drug products. Drug Discov. Today 8, 898–905.
Nielsen, L.S., Schubert, L., Hansen, J., 1998. Bioadhesive drug delivery systems. I. Characterisation of mucoadhesive properties of systems based on glyceryl mono-oleate and glyceryl monolinoleate. Eur. J. Pharm. Sci. 6, 231–239.
Owen, D.H., Katz, D.F., 1999. A vaginal fluid simulant. Contraception 59, 91–95.
Owen, D.H., Katz, D.F., 2005. A review of the physical and chemical properties of human semen and the formulation of a semen simulant. J. Androl. 26, 459–469.
Patterson, J.E., James, M.B., Forster, A.H., Lancaster, R.W., Butler, J.M., Rades, T., 2005. The influence of thermal and mechanical preparative techniques on the amorphous state of four poorly soluble compounds. J. Pharm. Sci. 94, 1998–2012.
Ren, Y., Yu, C., Meng, K., Tang, X., 2008. Influence of formulation and preparation process on ambroxol hydrochloride dry powder inhalation characteristics and aerosolization properties. Drug Dev. Ind. Pharm. 34, 984–991.
Stevens-Simon, C., Jamison, J., McGregor, J.A., Douglas, J.M., 1994. Racial variation in vaginal pH among healthy sexually active adolescents. Sex Transm. Dis. 21, 168–172.
Team, C.P.I.S.A.S., 2010. Expanded safety and acceptability of the candidate vaginal microbicide Carraguard(R) in South Africa. Contraception 82, 563–571.
Tevi-Benissan, C., Belec, L., Levy, M., Schneider-Fauveau, V., Si Mohamed, A., Hallouin, M.C., Matta, M., Gresenguet, G., 1997. In vivo semen-associated pH neutralization of cervicovaginal secretions. Clin. Diag. Lab. Immunol. 4, 367–374.
UNAIDS Report on the global AIDS epidemic 2011.
UNAIDS/WHO, 2011. Global HIV/AIDS Response-Epidemic Update and Health Sector Progress Towards Universal Access. UNAIDS, Geneva, p. 229.
Wan, L., Pooyan, S., Hu, P., Leibowitz, M.J., Stein, S., Sinko, P.J., 2007. Peritoneal macrophage uptake, pharmacokinetics and biodistribution of macrophage-targeted PEG-fMLF (N-formyl-methionyl-leucyl-phenylalanine) nanocarriers for improving HIV drug delivery. Pharm. Res. 24, 2110–2119.
Wang, Y.Y., Lai, S.K., Suk, J.S., Pace, A., Cone, R., Hanes, J., 2008. Addressing the PEG mucoadhesivity paradox to engineer nanoparticles that "slip" through the human mucus barrier. Angew. Chem. Int. Ed. Engl. 47, 9726–9729.
Whaley, K.J., Hanes, J., Shattock, R., Cone, R.A., Friend, D.R., 2010. Novel approaches to vaginal delivery and safety of microbicides: biopharmaceuticals, nanoparticles, and vaccines. Antiviral Res. 88 (Suppl 1), S55–S66.
Zhang, T., Sturgis, T.F., Youan, B.B., 2011. PH-responsive nanoparticles releasing tenofovir intended for the prevention of HIV transmission. Eur. J. Pharm. Biopharm. 79, 526–536.
Zidan, A.S., Spinks, C., Fortunak, J., Habib, M., Khan, M.A., 2010. Near-infrared investigations of novel anti-HIV tenofovir liposomes. AAPS J. 12, 202–214.